

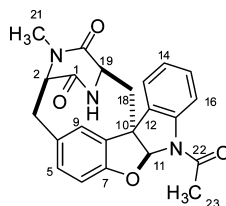
Azonazine, a Novel Dipeptide from a Hawaiian Marine Sediment-Derived Fungus, *Aspergillus insulicola*

Quan-Xiang Wu,^{†‡} Mitchell S. Crews,[‡] Marija Draskovic,[‡] Johann Sohn,[‡] Tyler A. Johnson,^{‡,⊥} Karen Tenney,[‡] Frederick A. Valeriote,[§] Xiao-Jun Yao,[†] Leonard F. Bjeldanes,[⊥] and Phillip Crews^{‡,*}

State Key Laboratory of Applied Organic Chemistry, College of Chemistry and Chemical Engineering, Lanzhou University, Lanzhou 730000, China, Department of Chemistry and Biochemistry, University of California Santa Cruz, California 95064, United States, Henry Ford Health System, Detroit, Michigan 48202, United States, and Department of Nutritional Sciences and Toxicology, University of California Berkeley, California 94720, United States
phil@chemistry.ucsc.edu

Received June 16, 2010 (Revised Manuscript Received September 10, 2010)

ABSTRACT



Azonazine, a unique hexacyclic dipeptide, was isolated from a Hawaiian marine sediment-derived fungus eventually identified as *Aspergillus insulicola*. Its absolute configuration, 2*R*,10*R*,11*S*,19*R*, was established using NMR, HRESIMS, and CD data plus insights derived from molecular models. A possible route for its biogenesis is proposed, and biological properties were explored against cancer cell lines and in an NFκB inhibition assay.

We believe that scientific study of fungi (Ascomycota) within the genus *Aspergillus* (Class: Eurotiomycetes, Family: Trichocomaceae) is important. Though more than 200 *Aspergillus* strains have been isolated from a host of terrestrial ecological niches, they provide a steady stream of diverse small molecules.¹ Recent genomics understanding of chemically prolific *Aspergillus* strains has emerged as sequences have been completed for eight *Aspergillus* species (*clavatus*, *flavus*, *fischeri*, *fumigatus*, *oryzae*, *nidulans*, *niger*, and *terreus*).² Results have also been obtained to correlate bioinformatic analysis to the operation of putative biosynthetic

gene clusters,³ in part,⁴ during the parallel study of their products observed under different culture conditions for three taxa from the preceding list.⁵

The use of OSMAC (One Strain *M*Any Compounds) to discover new biosynthetic products from *Aspergillus* is of particular interest to us and others.⁶ In this context, it is important to cite some small molecule natural products that can be considered as *Aspergillus*-derived landmarks, some

(2) Wortman, J. R.; Gilsenan, J. M.; Joardar, V.; Deegan, J.; Clutterbuck, J.; Turner, G.; et al. *Fungal Genet. Biol.* **2009**, *46*, S2–S13.

(3) Georgianna, D. R.; Fedorova, N. D.; Burroughs, J. L.; Dolezal, A. L.; Bok, J. W.; Horowitz-Brown, S.; Woloshuk, C. P.; Yu, J.; Keller, N. P.; Payne, G. A. *Mol. Plant Path.* **2010**, *11*, 213–226.

(4) Machida, M.; Gomi, K. *Aspergillus, Molecular Biology & Genomics*; Caister Academic Press: Norfolk, UK, 2010.

(5) Frisvad, J. C.; Smedsgaard, J.; Samson, R. A.; Larsen, T. O.; Thrane, U. *J. Agric. Food Chem.* **2007**, *55*, 9727–9732.

[†] Lanzhou University.

[‡] University of California Santa Cruz.

[§] Henry Ford Health System.

[⊥] University of California, Berkeley.

(1) Cole, R. J.; Jarvis, B. B.; Schweikert, M. A. *Handbook of Secondary Fungal Metabolites*; Academic Press: San Diego, 2003; Vols. I–III.

of which are also secondary metabolites from the eight full genome sequenced species. The top six among these are: (a) carcinogenic polyketides of the aflatoxin family (*A. flavus*),⁷ (b) medically important diterpenoids of the lovastatin family (*A. terreus*),⁸ (c) the mixed biogenesis mycotoxin cyclopiiazonic acid (*A. flavus* & *oryzae*),⁹ (d) NRPS peptides of the penicillin family (*A. nidulans*),¹⁰ (e) the widely bioactive diketopiperazines (DKPs) of the gliotoxin class (*A. fumigatus*),¹¹ and (f) products of commerce such as citric acid (*A. niger*).¹²

We began a campaign to emphasize chemical study on the >20 marine-derived *Aspergillus* strains (from sponges and sediments) housed in the UCSC repository. The prospect of encountering orphan¹³ biosynthetic pathways was part of the rationale for this investigation. The results reported below represent a first step and involve the characterization and biological evaluation of a novel hexacyclic dipeptide, azonazine from *A. insulicola* related to *ochraceopetaliformis* (syn: *A. flocculosisi*).¹⁴

This project was initiated by scanning our collection of *Aspergillus* cultures to identify those possessing strain uniqueness accompanied by activity in a cytotoxicity soft agar-based disk diffusion assay.¹⁵ One top candidate was *A. insulicola* (strain no. 088708a, identified by molecular taxonomy evaluations shown in Table S5, Supporting Information) obtained from a Hawaiian shallow water sediment. The EtOAc crude extract of the initial small-scale culture (125 mL, in Czapek-Dox liquid medium, pH adjusted to 7.0, prepared with artificial seawater) exhibited potent activity (see Table S2, Supporting Information) against murine colon 38 cell lines and selectivity against human prostate adenocarcinoma (LNCaP) vs human leukemia cell lines (CEM). A scale up culture (10 L, same media) was harvested at 21 days (shaking at 150 rpm) and worked up by passing it through HP-20 resin. The resin was subsequently washed using water (fraction coded: Hp1, 362 mg), 50% methanol/water (Hp2, 1327 mg), methanol (Hp3, 443 mg), and 2-propanol (Hp4, 12.8 mg). Each fraction was subjected to LCMS analysis and the Hp3 was selected for further purification via RP-HPLC (30–50% acetonitrile/0.1% formic acid–water, 50 min), and 42 fractions (F1–F42) were

collected. Further purification of fraction F11 (3.5 mg) via RP-HPLC yielded azonazine (1.1 mg) and insulicolide A (2.2 mg).¹⁶

Early on, we recognized that azonazine,¹⁷ obtained as a colorless powder and possessing molecular formula $C_{23}H_{21}N_3O_4$, was unique. This formula, based on the HRES-IMS quasimolecular ion at m/z 426.14160 [$M + Na$]⁺ (calcd 426.14243), was not found in dereplication searches of standard natural products databases. The UV absorption maximum at 239 nm implied the presence of aromatic functionality also evident in the NMR traces. The first hurdle in the azonazine characterization involved establishing the substructures responsible for the 15 units of unsaturation, consistent with the observation of only seven ¹³C NMR resonances in the aliphatic region (δ_C 20–75). Side-by-side inspection of the proton and carbon NMR spectra (see Table S1, Supporting Information) followed by obtaining gHMQC and the broadband-decoupled ¹³C NMR data eventually facilitated the drafting of several substructures. These contained 9 quaternary, 10 methine, 2 methylene, and 2 methyl carbons ($C_{23}H_{20}$). One additional proton (δ_H 7.04 brs) was eventually assigned as an NH group.¹⁸ Another essential observation included assigning the NMR resonances for three amide carbonyl carbons (δ_C 169.49, 165.51 and 171.34), an *N*CH₃ (δ_H 2.40 s, δ_C 32.83), two ABX patterns (δ_H 4.09/3.49/3.08; δ_H 4.26/2.84/2.49), and an *N*Ac group [δ_H 2.42 (3H, s), δ_C 171.34, 24.16].¹⁹

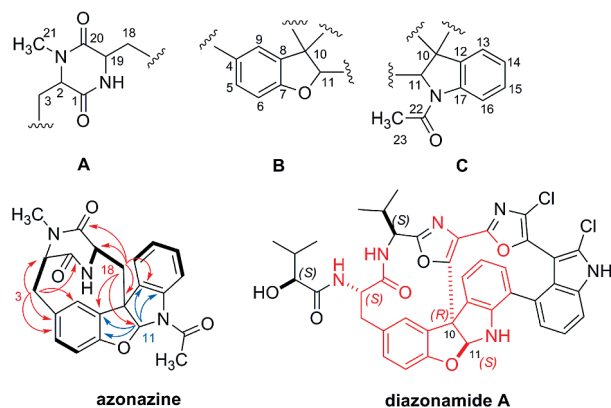


Figure 1. Substructures and key 2D NMR correlations.

Three substructures, A–C, shown in Figure 1, were assembled once the gCOSY and gHMBC (CD_3CN) data sets had been collected. The DKP, substructure A,²⁰ suspected from the outset based on occurrence of this residue in *Aspergillus* metabolites, was affirmed on the basis of the preceding data plus gCOSY correlations (Table S1, Supporting Information) between H18/H19/NH and diagnostic gHMBC correlations (H_3C_{21} to C2, C20; HN to C2, C20; H2 to C1, C3, C20, C21; and H19 to C1, C18, C20). The

(16) (a) Belofsky, G. N.; Jensen, P. R.; Renner, M. K.; Fenical, W. *Tetrahedron* **1998**, *54*, 1715–1724. (b) Rahbaek, L.; Christophersen, C.; Frisvad, J.; Bengaard, H. S.; Larsen, S.; Rassing, B. R. *J. Nat. Prod.* **1997**, *60*, 811–813.

(6) (a) Christian, O. E.; Compton, J.; Christian, K. R.; Mooberry, S. L.; Valeriote, F. A.; Crews, P. *J. Nat. Prod.* **2005**, *68*, 1592–1597. (b) Cichewicz, R. H. *Nat. Prod. Rep.* **2010**, *27*, 11–22.

(7) (a) Cole, R. J.; Cox, R. H. *Handbook of Toxic Fungal Metabolites*; Academic Press: New York, 1981; pp 15–19. (b) Cole, R. J.; Schweikert, M. A. *Handbook of Secondary Fungal Metabolites*; Academic Press: San Diego, 2003; Vol. I, pp 545–569.

(8) Sanchez, J. F.; Chiang, Y. M.; Wang, C. C. *Mol. Pharm.* **2008**, *5*, 226–233.

(9) Chang, P. K.; Ehrlich, K. C.; Fujii, I. *Toxins* **2009**, *1*, 74–99.

(10) (a) Dulaney, E. L. *Mycologia* **1947**, *39*, 570. (b) Dulaney, E. L. *Mycologia* **1947**, *39*, 582.

(11) (a) Johnson, J. R.; Bruce, W. F.; Dutcher, J. D. *J. Am. Chem. Soc.* **1943**, *65*, 2005–2009. (b) Balibar, C. J.; Walsh, C. T. *Biochemistry* **2006**, *45*, 5029–5038.

(12) Lewis, K. F.; Weinhouse, S. *J. Am. Chem. Soc.* **1951**, *73*, 2500–2503.

(13) Bok, J. W.; Hoffmeister, D.; Maggio-Hall, L. A.; Murillo, R.; Glasner, J. D.; Keller, N. P. *Chem. Biol.* **2006**, *13*, 31–37.

(14) Peterson, S. W. *Mycologia* **2008**, *100*, 205–226.

(15) Subramanian, B.; Nakeff, A.; Tenney, K.; Crews, P.; Gunatilaka, L.; Valeriote, F. A. *J. Exp. Ther. Oncol.* **2006**, *5*, 195–204.

dihydrobenzofuran, substructure **B**,²¹ was deduced on the basis of gCOSY correlations (H5 to H6) and gHMBC correlations (H5 to C7, C9; H6 to C4, C8; H9 to C5, C7, C10; and H11 to C7, C8). Finally, the *N*-Ac-dihydroindole, substructure **C**,^{19b} was drawn based on gCOSY correlations (between H13/H14/H15/H16) and gHMBC correlations (H13 to C10, C15, C17; H14 to C12, C16; H15 to C13, C17; H11 to C12, C17, C22; and H23 to C22). At this point, it was clear that the C10–C11 bond was common to substructures **B** and **C** and that the CH11 ($\delta_{\text{C/H}}$ 106.95/6.58) shifts were virtually identical to that of a similar residue (CH11 $\delta_{\text{C/H}}$ 106.1/6.35) in diazonamide A.^{21a,b} These data justified fusion of **B** and **C** via the benzofuro indole ring system (i.e., the bottom fused tetracyclic piece of diazonamide A). Reassuringly, all of the other the CH and C shifts for the dihydrobenzofuran of diazonamide A were virtually identical to those of azonazine. The final degree of unsaturation was accounted for by docking **A** at position C4 and C10, but there were two possible outcomes. The correct connectivity was deduced based on gHMBC correlations shown in Figure 1 (H3 to C4, C5, C9; H18 to C8, C10, C11, C12; and H11 to C7, C8, C12, C17, C18, C22). This assignment was also consistent with the NOE data.

With the gross structure of this novel peptide assembled, the elements of diazonamide A and the diketopiperazine core residue were used as the basis for the name, azonazine. The next step involved assigning the absolute configurations at each of the four chiral centers. Preliminarily, it was tempting to use the lack of ⁵*J* coupling between H2 and H19 as indication of their relative *anti*-orientation.²² However, a rigorous test of this prospect was provided by interpreting key 1D-NOE correlations shown in Figure 2 (also see Table

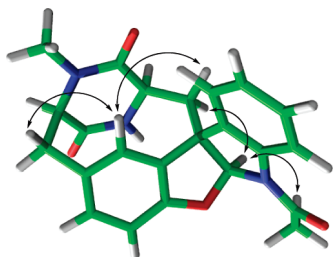


Figure 2. Energy-minimized conformation with key 1D-NOE correlations for azonazine.

S1 and Figure S15, Supporting Information). Correlations between H3b/H9 and H18a/H9 indicated that C3 and C18 were on the same facial plane. Furthermore, the intense correlation between H11 and H18b indicated a *cis* junction between the dihydrofuran ring and dihydropyrrole, which is identical to the ring fusion geometry in diazonamide A. Given these conclusions, it was possible to prune a longer list of possible candidate stereostructures to just those assembled in Figure 3, coded as **I–VI**. Model building of each via Chem3D energy minimization calculations provided some valuable insights (Table S4, Supporting Information). Initial qualitative evaluation of these structures suggested

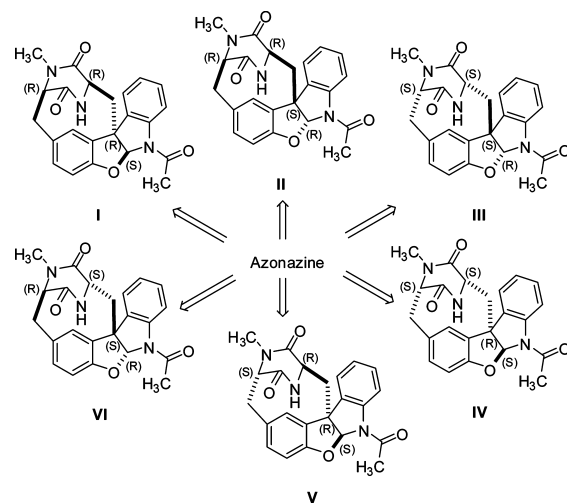


Figure 3. Matrix of possible azonazine configurations.

that **II** and **IV** possessed significant intra ring strain; consequently, attention was shifted to further scrutiny of the others.

Our next task, to evaluate the other viable candidates, **I**, **III**, **V**, and **VI** was guided by comparing the actual electronic circular dichroism (ECD) trace of azonazine with those predicted using time-dependent density functional theory (TD-DFT) calculations.²³ This approach is becoming a powerful tool in the absolute configuration analysis of natural products.²⁴ Azonazine displayed a trio of positive Cotton effects (CEs) at 220, 255, and 300 nm and a negative CE inflection at 240 nm as shown in Figure 4. This trace was directly compared to those obtained by calculation for the optimized geometries of each structure using the B3LYP/6-31G(d) forcefield annotated for methanol solution. An

(17) UV (MeOH) λ_{max} (log ϵ) 204.0 (5.58), 239.0 (5.14), 287.0 (4.56) nm; $[\alpha]_{\text{D}}^{25} +295.0$ (c 0.1, MeOH); ¹HNMR (600 MHz, CD₃CN) δ_{H} 4.09 (d, *J* = 7.2, H-2), 3.08 (dd, *J* = 14.4, 7.2, H-3a), 3.49 (d, *J* = 14.4, H-3b), 6.95 (dd, *J* = 7.8, 1.2, H-5), 6.67 (d, *J* = 8.4, H-6), 7.50 (s, H-9), 6.58 (s, H-11), 7.59 (d, *J* = 7.2, H-13), 7.19 (t, *J* = 7.8, H-14), 7.29 (t, *J* = 7.8, H-15), 8.13 (brs, *J*_{w/2} = 7.8, H-16), 2.49 (dd, *J* = 16.8, 1.8, H-18a), 2.84 (dd, *J* = 16.8, 5.4, H-18b), 4.26 (d, *J* = 5.4, H-19), 2.40 (s, H-21), 2.42 (s, H-23), 7.04 (brs, NH); ¹³CNMR (150 MHz, CD₃CN) δ_{C} 169.49 (s, C-1), 66.26 (d, C-2), 39.21 (t, C-3), 133.20 (s, C-4), 131.51 (d, C-5), 110.83 (d, C-6), 158.99 (s, C-7), 131.98 (s, C-8), 126.42 (d, C-9), 59.06 (s, C-10), 106.95 (d, C-11), 135.34 (s, C-12), 124.13 (d, C-13), 125.72 (d, C-14), 129.61 (d, C-15), 117.29 (d, C-16), 142.48 (s, C-17), 43.35 (t, C-18), 54.80 (d, C-19), 165.51 (s, C-20), 32.83 (q, C-21), 171.34 (s, C-22), 24.16 (q, C-23).

(18) Amagata, T.; Morinaka, B. I.; Amagata, A.; Tenney, K.; Valeriote, F. A.; Lobkovsky, E.; Clardy, J.; Crews, P. *J. Nat. Prod.* **2006**, *69*, 1560–1565.

(19) (a) Boot, C. M.; Amagata, T.; Tenney, K.; Compton, J. E.; Pietraszkiwicz, H.; Valeriote, F. A.; Crews, P. *Tetrahedron* **2007**, *63*, 9903–9914. (b) Minatti, A.; Buchwald, S. L. *Org. Lett.* **2008**, *10*, 2721–2724.

(20) (a) Watts, K. R.; Ratnam, J.; Ang, K. -H.; Tenny, K.; Compton, J. E.; McKerrow, J.; Crews, P. *Bioorg. Med. Chem.* **2010**, *18*, 2566–2574. (b) Kozlovsky, A. G.; Vinokurova, N. G.; Adanin, V. M.; Burkhardt, G.; Dahse, H. M.; Gräfe, U. *J. Nat. Prod.* **2000**, *63*, 698–700.

(21) (a) Lindquist, N.; Fenical, W. *J. Am. Chem. Soc.* **1991**, *113*, 2303–2304. (b) Fernández, R.; Martín, M. J.; Rodríguez-Acebes, R.; Reyes, F.; Francesch, A.; Cuevas, C. *Tetrahedron Lett.* **2008**, *49*, 2283–2285. (c) Fuerst, D. E.; Stoltz, B. M.; Wood, J. L. *Org. Lett.* **2000**, *2*, 3521–3523.

(22) Varoglu, M.; Corbett, T. H.; Valeriote, F. A.; Crews, P. *J. Org. Chem.* **1997**, *62*, 7078–7079.

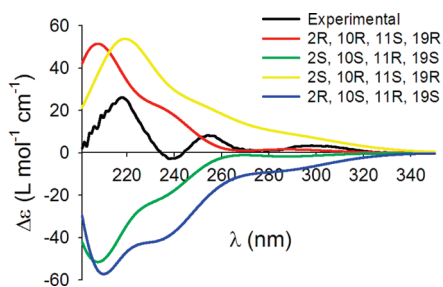


Figure 4. Experimental CD spectrum of azonazine overlaid with calculated spectra for structures shown in Figure 3: (2*R*,10*R*,11*S*,19*R*)-**I**, (2*S*,10*S*,11*R*,19*S*)-**III**, (2*S*,10*R*,11*S*,19*R*)-**V**, and (2*R*,10*S*,11*R*,19*S*)-**VI**.

overview of our conclusions based on these and other considerations are summarized in Table S4, Supporting Information. The matchup between the experimental and that calculated for structure **I** was excellent as can be seen from comparison to the predicted positive CEs at 210, 240, and 290 nm. Similar, but not quite perfect, agreement was seen with the CD calculated for **V** exhibiting an intense positive CE at 220 nm. The negative CEs predicted for **III** and **VI** allowed these structures to be ruled out.

At this juncture, the list of viable configuration candidates consisted of **I**, **II**, **IV**, and **V**. Analysis of the diagnostic 1D-NOE correlations indicated that all four structures provided a fit for the data (Table S4, Supporting Information). However, there is a substantial difference in the δ Hs for aryl protons H9 (δ 7.50) vs H5 (δ 6.95). Insights from the MMX models shown in Figure S15a (Supporting Information) show that these protons have a different anisotropic environment due to the different DKP carbonyl group shielding for structures **I** and **II** but this is not observable for **IV** and **V**. Thus, the latter pair was ruled out for further consideration.

There appear to be some unique biosynthetic reactions operating to assemble the chirality and substitution patterns present in (+)-azonazine. A retro-assembly analysis predicts that D-Tyr and D-Trp undergo additional functionalization prior to condensation generating the DKP of either **I** or **II**. An electrocyclic-like process proceeding in a stereospecific fashion can be envisaged to generate the other rings (Figure S16, Supporting Information).²⁵ It appears that a similar reaction cascade operates to form the central rings possessing R10 and S11 (of **I**) or S10 and R11 (of **II**). We favor

assigning absolute configuration of azonazine in parallel to that of diazonamide (*R*10/*S*11), and proposed the configuration of **I** as 2*R*,10*R*,11*S*,19*R*.

The cytotoxicity of the crude extract containing azonazine encouraged our view that it might have parallel activity vs that diazonamide A (i.e., IC₅₀ values <15 ng/mL against HCT-116).^{21a} Bioassay-guided fractionation (Hp3) revealed insulicolide A¹⁶ as the solid tumor selective agent (see Tables S2 and S3 and Chart S1, Supporting Information). Further testing showed that azonazine was inactive at 1 mg/mL in the disk diffusion assay and it was inactive using an MTT screen²⁶ at 100 μ M against human prostate (PC3), human breast adenocarcinoma (MCF-7), and murine macrophage (RAW 264.7) cells. Alternatively, azonazine exhibited anti-inflammatory activity (see Figure S17, Supporting Information) by inhibiting NF- κ B luciferase (IC₅₀ 8.37 μ M) and nitrite production (IC₅₀ 13.70 μ M) but was less potent than the standard celastrol (IC₅₀ 0.3 μ M).²⁷

Acknowledgment. Support was received from NIH Grant Nos. CA 47135 (PC), CA 052955 (PC), FIC/NIH u01TW008160 (LFB) and fellowships from China, 2007CB108903, and Lanzhou University (LZUJC2007005). UT San Antonio (Dr. Thompson & Dr. Wickes) provided taxonomic results.

Supporting Information Available: Extraction scheme and bioactivity data, NMR data, possible configurations, and biosynthetic pathway of azonazine. This material is available free of charge via the Internet at <http://pubs.acs.org>.

OL101396N

(23) (a) Bringmann, G.; Bruhn, T.; Maksimenka, K.; Hemberger, Y. *Eur. J. Org. Chem.* **2009**, 2717–2727. (b) Ding, Y.; Li, X. C.; Ferreira, D. *J. Org. Chem.* **2007**, 72, 9010–9017. (c) Berova, N.; Bari, L. D.; Pescitelli, G. *Chem. Soc. Rev.* **2007**, 36, 914–931. (d) Stephens, P. J.; McCann, D. M.; Devlin, F. J.; Cheeseman, J. R.; Frisch, M. J. *J. Am. Chem. Soc.* **2004**, 126, 7514–7521. (e) Stephens, P. J.; McCann, D. M.; Butkus, E.; Stoncius, S.; Cheeseman, J. R.; Frisch, M. J. *J. Org. Chem.* **2004**, 69, 1948–1958. (f) McCann, D. M.; Stephens, P. J. *J. Org. Chem.* **2006**, 71, 6074–6098.

(24) (a) Yang, X. W.; Ding, Y.; Li, X. C.; Ferreira, D.; Shen, Y. H.; Li, S. M.; Wang, N.; Zhang, W. D. *Chem. Commun.* **2009**, 3771–3773. (b) Wu, X. F.; Hu, Y. C.; Yu, S. S.; Jiang, N.; Ma, J.; Tan, R. X.; Li, Y.; Lv, H. N.; Liu, J.; Ma, S. G. *Org. Lett.* **2010**, 12, 2390–2393.

(25) (a) Li, J.; Burgett, A. W. G.; Esser, L.; Amecdzua, C.; Harran, P. G. *Angew. Chem., Int. Ed.* **2001**, 40, 4770–4773.

(26) Wu, Q. X.; Yang, A. M.; Shi, Y. P. *Tetrahedron* **2005**, 61, 10529–10535.

(27) (a) Gilmore, T. D. *Oncogene* **2006**, 25, 6680–6684. (b) Naylor, L. H. *Biochem. Pharmacol.* **1999**, 58, 749–757. (c) Tachibana, M.; Matsui, C.; Takeuchi, Y.; Suzuki, E.; Umezawa, K. *Heterocycles* **2008**, 76, 1561–1569. (d) Jin, H. Z.; Hwang, B. Y.; Kim, H. S.; Lee, J. H.; Kim, Y. H.; Lee, J. J. *J. Nat. Prod.* **2002**, 65, 89–91.